Parameter Trade-Off in One-Dimensional Magnetotelluric Modelling

G. Fischer and B.V. Le Quang

Observatoire Cantonal, CH-2000 Neuchâtel, Switzerland

Abstract. The problem of inverting or modelling one-dimensional magnetotelluric data can, today, be considered as largely resolved. Attention now focuses on the class of acceptable models. Viewed in the space of model parameters this class occupies a singly connected volume, bound with a surface where the standard deviation ε between measured and calculated response exceeds the minimum ε_0 of the best-fitting model by a constant factor (typically $\varepsilon \cong 1.10\, \varepsilon_0$). This volume of acceptable models is described by its intersections with the parameter axes, and also by the extreme excursions possible for any of the model parameters when all the other parameters are adjusted accordingly. These extreme excursions therefore represent "trade-off" conditions among the model parameters and are summarized in the "trade-off matrix". In a sense this is a generalization of the parameter correlation matrix, which gives only local information in the vicinity of a proposed model. The trade-off matrix, however, is independent of any initial model. Another important question considered deals with the correct choice of the number of layers with which to model a data set. Whereas a single minimum of ε is found with the correct number n_0, when this number is too small the information contained in the data is spread among several isolated minima. When $n > n_0$ the problem becomes "ill-posed". There are too many degrees of freedom and it becomes possible, then, to move in model space in directions at right angles to the meaningful dimensions without finding a clear minimum. The problem is analogous to a vanishing determinant in linear algebra. To find a regular problem again it is necessary to specify auxiliary constraints provided, for example, by other soundings or prior geological knowledge, to compensate for the increased number of variables.

Key words: Parameter trade-off in 1 D/MT – Magnetotelluric modelling – Degrees of freedom in geophysical inversion

The Concept of Acceptable Models

The last two or three years have seen many new schemes with which to invert or model one-dimensional (1 D) magnetotelluric (MT) sounding results (Shoham et al., 1978; Jones and Hutton, 1979; Oldenburg, 1979; Parker, 1980; Parker and Whaler, 1981; Larsen, 1981; Eichler, 1980; Fischer et al., 1981; Fischer and Le Quang, 1981; Hobbs, 1982). If it is safe to assert, today, that the best-fitting 1 D model to a given MT data set can usually be found, the same cannot be said as regards the family of models compatible with this set. By this criterion of compatibility we mean the ensemble of models yielding response functions which lie within a certain range of the standard deviation $\varepsilon_0 = \varepsilon_{\min}$ of the best-fitting model. In what follows the standard deviation ε defined by Fischer et al. (1981) will be used. For data points with uniform weights this definition reduces to

$$
\varepsilon = \frac{1}{\sqrt{2}} (\varepsilon_\rho^2 + \varepsilon_\phi^2)^{1/2}
$$
$$
= \frac{1}{\sqrt{2}} \left[\frac{1}{N} \sum_{i=1}^{N} |\ln Z_c(T_i) - \ln Z_m(T_i)|^2 \right]^{1/2} \tag{1}
$$

where $Z_c(T_i)$ and $Z_m(T_i)$ refer to calculated and measured impedances at the N measurement periods T_i.

The data are generally given in terms of apparent resistivity $\rho_a(T_i)$ and phase $\phi(T_i)$, such that

$$
Z_m(T_i) = \sqrt{2 \pi \mu_0 \rho_a(T_i)/T_i} \, \exp\left\{ i \left[\frac{\pi}{4} - \phi(T_i) \right] \right\}. \tag{2}
$$

If the data points $\rho_a(T_i)$ and $\phi(T_i)$ are given weights, which may appropriately be chosen as inversely proportional to the error ranges of the data, it becomes necessary to compute ε_ρ and ε_ϕ separately, along the lines proposed by Fischer et al. (1981). The separation of ε_ρ and ε_ϕ clearly suggests that it is also possible to model sets with different numbers of $\rho_a(T_i)$ and $\phi(T_i)$ data points, in particular data sets consisting only of apparent resistivity measurements. When this happens the quality of the fit is appraised in terms of ε_ρ alone.

The idea of asking for the family of models compatible with the measured data has at least two quite different origins. Looking at the smooth response function of the best-fitting model traced through the measured data, one is led quite naturally to ask about the family of models yielding an almost equally good fit. Quantifying the notion of "almost equally good fit" is not too difficult, since it is usually quite easy to distinguish models whose response yields a misfit which is 20% above ε_0, whereas an increase of only 10% is barely noticeable, or not noticeable at all.

Offprint requests to: G. Fischer

SITE 4

BEST-FITTING MODEL $\varepsilon_p = 0.0693$
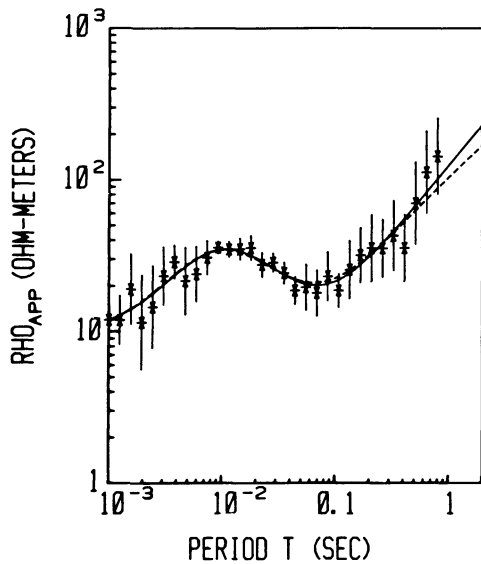MOST ACCEPTABLE MODEL $\varepsilon_p = \underline{0.0754}$

Fig. 1. MT data for the SITE 4 station (Schnegg et al., 1982). Only the apparent resistivity has been modelled. The solid line corresponds to the best-fitting model (Tables 1 or 2), the dashed line belongs to a geologically acceptable model

MODELLING WITH VARIOUS VALUES OF ρ_3
SITE 4

Fig. 2. Trade-off relationship between ρ_3 and h_3 for the data from SITE 4 station (cf. Fig. 1)

This 10% limit is admittedly somewhat arbitrary, but the arguments that follow are independent of the choice of this limit, which could equally well be set at another value. Henceforth, however, a model will be deemed acceptable if its standard deviation lies within the range of a 10% increase over the best-fitting value ε_0.

An entirely different approach to the notion of acceptable model arises when the best-fitting model obtained via the minimization of ε is compared with the geological structure to which the sounding data refer. Certain parameters of the structure under MT investigation may be quite well known already from other studies. The question then arises whether these known parameters can be fitted into a compromise model whose response remains within the acceptable range of 1.10 ε_0. This second point of view brings the trade-off notion to the fore, inasmuch as it is generally quite possible to find an acceptable model agreeing with the known geological parameters, provided the permissible range of the remaining model parameters is reduced. An example of this trade-off notion can be given in relation to the data set of Fig. 1 (Schnegg et al., 1982). The best-fitting model to these $\rho_a(T)$ data comprises a lowest or fourth layer with $\rho_4 = 10^4$ Ωm. In fact the modelling process would even yield a slightly higher resistivity, but the model search is restricted by the following arbitrarily set bounds: $0.1 \leqq \rho_j \leqq 10^4$ Ωm, $h_k \geqq 1$ m. In this particular sounding the fourth layer refers to a well-known limestone base, with large areas nearby where it reaches the surface. Its electrical resistivity is therefore well established by other methods such as laboratory measurements and geoelectrical soundings, and a value of 1,200 Ωm is generally favoured. Furthermore, the third layer is a thin highly conducting marl formation, whose thickness does not exceed 20 m. Is it possible to find an acceptable model with prescribed parameter
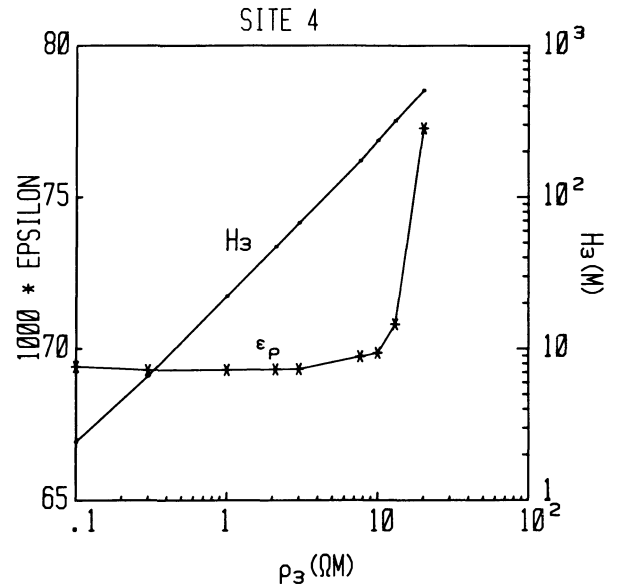
values of $\rho_4 = 1,200$ Ωm and $h_3 = 0.020$ km? As seen in Figs. 1 and 2 and Table 2 this is perfectly feasible, provided the value of ρ_3 is reduced to about 1 Ωm. In this particular case all that seems to matter is the layer conductance $h_3/\rho_3 \simeq 20$–25 mho, as long as ρ_3 remains below about 10 Ωm and h_3 below 200 m. But the trade-off process is connected with an obvious gain: prescribing the thickness h_3 of the marl formation reduces the uncertainty of its resistivity ρ_3.
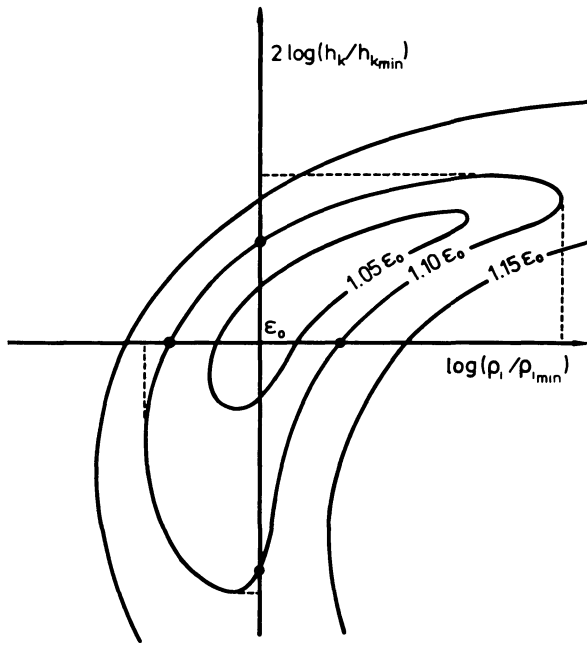
The Trade-Off Surface

The modelling process is conveniently described in the space of model parameters with logarithmic coordinates:

$$x_j = \log_{10}(\rho_j/\rho_{j0}),$$
$$y_k = 2 \log_{10}(h_k/h_{k0}). \tag{3}$$

ρ_{j0} and h_{k0} referring at first to the initial model chosen. The minimization of ε is carried out by a search routine which plays on the various model parameters, seeking the coordinates of the point with the lowest $\varepsilon = \varepsilon_0$ (Fischer and Le Quang, 1981). The search strategy generally does not attempt to determine the most appropriate number n_0 of layers. But this number is easily obtained by looking at the ε_0 values achievable with various numbers of layers. Figure 11, pertaining to the four examples chosen, clearly shows that for $n < n_0$, a rapid increase of ε_0 occurs, whereas ε_0 usually remains almost constant when $n > n_0$. The importance of determining the correct number n_0 will be dealt with in a later section.

Once n_0 and the coordinates of the best-fitting model have been secured it is convenient to move the origin of the space of model parameters to this point. As the various examples will show, this point, now with coordinates (ρ_{j0}, h_{k0}), does not necessarily correspond to the absolute

Fig. 3. Example of trade-off surface in two dimensions. The intersections with the axes correspond to the *partial sensitivity matrix* data, whereas the coordinates of the extreme excursions in the direction of the axes yield the *trade-off matrix* data

minimum of ε; the reason for this is related to the bounds mentioned already for the family of acceptable models. It often happens that the true absolute minimum of ε would trespass these bounds, generally leading toward 0 or $+\infty$ for ρ_j and toward 0 for h_k.

Except for directions connected with the above-mentioned bounds, it is clear that, moving away from (ρ_{j0}, h_{k0}) in any direction of model parameter space, ε will be seen to increase above its minimum value ε_0. Under the condition that n_0 has been chosen correctly, Fischer and Le Quang (1981) have shown that this increase is very smooth, even though there is generally a high degree of anisotropy. But the surface corresponding to a 10% increase of ε, i.e. the $\varepsilon = 1.10 \, \varepsilon_0$ surface, is a well-defined entity. A graphical example in only two dimensions is shown in Fig. 3. Inside this surface is the entire collection of models with standard deviations $\varepsilon \leqq 1.10 \, \varepsilon_0$, and the question springs to mind whether this collection comprises any structures whose parameters are in accord with geological facts known already. Unless the sounding has been strongly perturbed by unwanted signals, it is quite probable that there will be such models among the acceptable collection, and these models will constitute a sub-class whose other parameters are generally more constrained than those of the entire collection. In other words, there will be a trade-off between the parameters of which the permitted range is strongly limited by the known geology, and all the remaining parameters. It is fair, therefore, to look at the $\varepsilon = 1.10 \, \varepsilon_0$ surface as the *trade-off surface*, enclosing a volume which will be called the *trade-off volume*. More rigorously speaking, ε is a $2n$ dimensional surface in parameter space and $\varepsilon = 1.10 \, \varepsilon_0$ in effect represents a trade-off contour, enclosing the trade-off surface element.

The *trade-off surface* must be expected to have a complicated structure. Fischer and Le Quang (1981) have shown that in certain directions of parameter space ε increases very fast, whereas there are curved valleys at the bottom of which ε remains close to ε_0 over very long distances. While it may be difficult to describe the *trade-off surface* in detail, two information sets can be given. Visualizing the *trade-off surface* as in Fig. 3 we may ask, first, about its intersections with the parameter axes as defined by Eq. (3). Approximate values of these intersections are listed in Tables 1, 3, and 5 for three data sets chosen as examples in the present study. These Tables, which we call *partial sensitivity matrices*, are obtained by calculating ε for models in which all parameters, except one, retain the coordinates of the minimum ε_0. The parameter singled out is progressively varied until ε reaches the limiting value $\varepsilon = 1.10 \, \varepsilon_0$. The corresponding parameter value is recorded in the *partial sensitivity matrix*. A graphical representation of the matrix is shown in Fig. 7, the *trade-off diagram*. In both Fig. 7 and *partial sensitivity matrices*, the parameters are increased to the right and decreased to the left.

Table 1. *Partial sensitivity matrix* for the SITE 4 data. Apparent resistivities are given in Ωm and thicknesses in km. All these models yield $\varepsilon_\rho = 1.10 \, \varepsilon_{\rho 0} = 76.25 \cdot 10^{-3}$, except the lowest right one where ε_ρ^0 remains at the value ε_ρ^0 because of the bound on ρ_4

11.0	$\rho_{10} = 11.9$	13.0
0.0375	$h_{10} = 0.0425$	0.0476
67.0	$\rho_{20} = 83.4$	111
0.289	$h_{20} = 0.321$	0.359
1.88	$\rho_{30} = 2.10$	2.35
0.0420	$h_{30} = 0.0470$	0.0525
1540	$\rho_{40} = 10^4$	10^4

$$\varepsilon_\rho^0 = 69.32 \cdot 10^{-3}$$

Table 2. *Trade-off matrix* for the SITE 4 data. Apparent resistivities are given in Ωm and thicknesses in km. The values of ε are also given; they are close to $1.10 \, \varepsilon_0$, except when a bound is reached, in which case they are usually close to ε_0

$\varepsilon_{\rho-}$ (10^{-3})	ρ_4	h_3	ρ_3	h_2	ρ_2	h_1	ρ_1		ρ_1	h_1	ρ_2	h_2	ρ_3	h_3	ρ_4	$\varepsilon_{\rho+}$ (10^{-3})
76.8	10^4	0.0362	1.59	0.352	88.7	0.001	<u>0.357</u>	$\rho_1 = 11.9$	<u>18.2</u>	0.0996	1830	0.258	1.76	0.0425	10^4	76.3
70.3	10^4	0.0642	3.02	0.368	56.9	<u>0.001</u>	0.468	$h_1 = 0.0425$	18.0	<u>0.104</u>	10^4	0.269	0.797	0.0193	10^4	76.5
76.3	10^4	0.0591	3.07	0.398	<u>42.8</u>	0.001	0.614	$\rho_2 = 83.4$	14.5	0.0739	<u>10^4</u>	0.276	1.66	0.0409	10^4	69.4
76.2	10^4	0.460	17.8	<u>0.146</u>	10^4	0.0519	12.6	$h_2 = 0.321$	2.19	0.00427	48.0	<u>0.444</u>	0.100	0.00189	10^4	76.5
69.4	10^4	0.00244	<u>0.100</u>	0.290	1200	0.0734	14.6	$\rho_3 = 2.10$	9.85	0.0386	2080	0.154	<u>19.1</u>	0.494	10^4	76.3
76.5	10^4	<u>0.00177</u>	0.100	0.413	47.2	0.00881	4.36	$h_3 = 0.0470$	9.22	0.0356	10^4	0.154	18.8	<u>0.499</u>	10^4	76.2
76.4	<u>1150</u>	0.0480	2.31	0.307	90.2	0.0430	11.9	$\rho_4 = 10^4$	11.9	0.0423	83.2	0.322	2.10	0.0470	<u>10^4</u>	69.3

$$\varepsilon_\rho^0 = 69.32 \cdot 10^{-3}$$

Table 3. *Partial sensitivity matrix* for station AHA (data courtesy of Jödicke 1980a). Apparent resistivities are given in Ωm and thicknesses in km. All these models yield $\varepsilon = 1.10\,\varepsilon_0 = 27.79 \cdot 10^{-3}$

2.62	$\rho_{10} = 2.69$	2.77
2.67	$h_{10} = 2.83$	2.98
19.6	$\rho_{20} = 34.6$	218
3.77	$h_{20} = 4.11$	4.48
1.28	$\rho_{30} = 1.39$	1.51
4.64	$h_{30} = 5.18$	5.77
10.8	$\rho_{40} = 16.5$	26.8

$$\varepsilon_0 = 25.27 \cdot 10^{-3}$$

Table 5. *Partial sensitivity matrix* for station NEW (data courtesy of Jones and Hutton, 1979). Apparent resistivities are given in Ωm and thicknesses in km. All these models yield $\varepsilon = 1.10\,\varepsilon_0 = 59.77 \cdot 10^{-3}$, except the uppermost right one where ε remains at the value ε_0 because of the bound on ρ_1

870	$\rho_{10} = 10^4$	10^4
11.7	$h_{10} = 13.5$	15.3
89.9	$\rho_{20} = 96.5$	103
43.9	$h_{20} = 49.0$	54.8
455	$\rho_{30} = 626.2$	928
218	$h_{30} = 270.9$	346
2.53	$\rho_{40} = 35.3$	146

$$\varepsilon_0 = 54.34 \cdot 10^{-3}$$

In most instances, however, it is possible to vary a given parameter beyond the limits corresponding to the intersections between *trade-off surface* and parameter axis, *if appropriate variations of the other parameters are permitted*. Figure 3 gives an illustration of this statement. This leads to the concept of *trade-off matrix*, of which three examples are given in Tables 2, 4 and 6. These tables are again obtained by imposing a progressive variation to a single selected parameter; this time, however, all the other parameters are adjusted freely with the minimization routine (Fischer and Le Quang, 1981) in order to reduce ε to the lowest possible value, under the two constraints of the single *imposed* variation and the bounds described before. The extremal parameter sets for which it is possible to find models which satisfy $\varepsilon \simeq 1.10\varepsilon_0$ are again listed in the *trade-off matrices*, the underlined diagonal elements of which are the extreme excursions possible for the selected parameter (minimum at left, maximum at right). These coordinate sets represent the projections on the parameter axes of the extreme extensions of the *trade-off surface*, according to the illustration shown in Fig. 3. Clearly the *trade-off matrix* tells us under what trade-off conditions a particular parameter may be given a pre-determined value. The *trade-off diagram* of Fig. 7, on the other hand, only contains part of the *trade-off matrix* information. What the *trade-off matrix* does not attempt to answer is under what conditions more than one parameter may be pegged to pre-determined value. However, such questions present no problem to our search routine, which can be programmed to seek the best-fitting model under a great variety of prescribed conditions, as shown in the following paragraph.

For the structure concerning the first example, several geological parameters are known already: $\rho_2 \simeq 80\ \Omega$m, $h_3 \leqq$ 20 m, and $\rho_4 \simeq 1,200\ \Omega$m. As seen in Fig. 1 these factors can easily be accommodated with the condition $\varepsilon \leqq 1.10\ \varepsilon_0$. The best model with fixed parameter values $h_3 = 20$ m and $\rho_4 = 1,200\ \Omega$m (since ρ_2 had been found in the correct range around $80\ \Omega$m, it was not fixed) that our search routine returned, yields $\varepsilon = 0.0753$ with $\rho_1 = 10.6\ \Omega$m, $h_1 = 34.9$ m, $\rho_2 = 76.0\ \Omega$m, $h_2 = 330$ m, and $\rho_3 = 0.985\ \Omega$m. This model corresponds to the dashed line in Fig. 1, which seems to fit the data no less well than the solid line of the best possible four-layer model, whose $\varepsilon = \varepsilon_0 = 0.0693$.

The term trade-off, as used in the present paper, describes compromise relationships among the model parameters which have to be obeyed when attempting to bring one or more of these parameters into some predetermined ranges. This meaning differs from the standard usage of the term trade-off in inversion theory, as employed also for induction or MT studies by Parker (1970) and Hobbs (1977). The standard trade-off diagrams express, at any given depth z, the accuracy with which the conductivity $\sigma(z)$ is resolved, in particular they show that resolving power and parameter stability cannot be maximized simultaneously: the term trade-off thus applies to the relation between these two concepts rather than to the model parameters themselves.

Our approach to the determination of the range of possible models is more closely related to the method of Single Value Decomposition (SVD) proposed by Lanczos (1961) and applied in various forms by many others (Wiggins, 1972; Jackson, 1973; Jupp and Vozoff, 1975; Vozoff and Jupp, 1975; Johansen, 1977; Edwards et al., 1981; and Rokityansky, 1982), or to the ridge regression of Inman (1975). In these methods a fit indicator ε in model space is studied in detail around a predetermined initial model.

Table 4. *Trade-off matrix* for station AHA (data courtesy of Jödicke 1980a). Apparent resistivities are given in Ωm and thicknesses in km. The values of ε are also given; they are close to $1.10\,\varepsilon_0$, except when a bound is reached, in which case they are usually close to ε_0

ε_- (10^{-3})	ρ_4	h_3	ρ_3	h_2	ρ_2	h_1	ρ_1		ρ_1	h_1	ρ_2	h_2	ρ_3	h_3	ρ_4	ε_+ (10^{-3})
27.82	16.5	4.00	1.24	6.50	6.19	1.51	<u>2.37</u>	$\rho_1 = 2.69$	<u>2.91</u>	3.40	167	4.25	1.04	3.77	17.4	27.83
27.77	17.5	3.72	1.17	6.83	5.89	<u>1.46</u>	2.39	$h_1 = 2.83$	2.89	<u>3.58</u>	10^4	5.08	0.335	1.14	16.5	27.81
27.82	16.9	3.32	1.07	7.03	<u>5.70</u>	1.49	2.44	$\rho_2 = 34.6$	2.70	2.94	<u>10^4</u>	3.81	1.42	5.38	16.4	25.22
27.96	25.3	10.8	2.39	<u>2.70</u>	436	2.56	2.62	$h_2 = 4.11$	2.46	1.53	5.76	<u>8.07</u>	0.345	0.978	18.4	27.66
25.65	13.3	0.318	<u>0.100</u>	5.34	1240	3.21	2.75	$\rho_3 = 1.39$	2.62	2.56	102	2.87	<u>2.41</u>	11.0	30.2	27.81
25.64	13.3	<u>0.313</u>	0.100	5.58	34.4	3.05	2.75	$h_3 = 5.18$	2.62	2.59	446	2.84	2.38	<u>11.3</u>	35.5	27.80
27.85	<u>8.14</u>	2.46	0.825	4.36	154	2.93	2.67	$\rho_4 = 16.5$	2.69	2.77	66.0	3.42	2.02	9.22	<u>53.5</u>	27.77

$$\varepsilon_0 = 25.27 \cdot 10^{-3}$$

The contour of acceptable models is something like a hyperellipsoid, whose orientation defines a set of new coordinates, each of which in general involves several or all of the original coordinates (the model parameters). Since the center of the hyperellipsoid is fixed it gives information on the topography of ε around that predetermined point; in particular if the model is located in a deep curving valley, the orientation of the valley floor will determine one of the hyperellipsoid axes.

The method presented in this paper is conceptually simpler than those quoted above, but it is more general. It has become possible to implement this simple approach only because we dispose of an efficient minimization program capable of returning the best-fitting model in only a few seconds of computing time. The search strategy moves from model to model and is not tied to a predetermined initial point in the space of parameters. Our *trade-off* and *partial sensitivity matrices* thus describe the surface bounding the acceptable models in much more general terms, and it is for convenience only that the best-fitting model, with $\varepsilon = \varepsilon_0$, is chosen as origin. By contrast, the hyperellipsoid gives *local* information about the shape of the *trade-off surface*, which, as shown by Fischer and Le Quang (1981) is in general highly anisotropic with a long curved valley close to the level of the lowest ε values. If the initial model is not within the range of the deep valley, the hyperellipsoid will be unable to yield any information on the orientation of the valley.

The *trade-off surface* defined in the present paper is not dependent on any linearization and its topology is not affected by the correct choice of an initial model. Choosing a model away from the true best fit simply increases the value of ε at the trade-off surface to a value slightly larger than $1.10\,\varepsilon_0$. But this is unlikely to change the general shape of the *trade-off surface*. The *trade-off matrix* may constitute a more "brute-force" approach to parameter trade-off, but it is more general than the SVD technique.

Some Typical Trade-Off Conditions

For electric or electromagnetic soundings to be capable of yielding geologically interesting information, the structure under study must exhibit reasonably large resistivity contrasts. This is true in particular for MT soundings. Restricting our attention to 1 D configurations, the above statement implies that structures with layers of alternately high and low resistivities are especially suitable for MT investigation.

Consider a good conductor, as for example layer 3 of

the first example (Fig. 1), sandwiched between the resistive layers 2 and 4. This is probably the most familiar trade-off situation in MT. If indeed ρ_2/ρ_3 and $\rho_4/\rho_3 \geqq 10$ and if the third layer thickness h_3 is sufficiently large, the apparent resistivity $\rho_a(T)$ will approach its extreme negative slope, i.e. $d \ln \rho_a(T)/d \log_{10} T \to -2.303$ over a certain range of periods, as seen in Fig. 1. This is the transition zone in which $\rho_a(T)$ is controlled mainly by the two resistivities ρ_2 and ρ_3. In the Fig. 1 example this range covers the periods from about 13–50 ms. No further change of slope will occur if ρ_3 is decreased by any constant factor $c > 1$. The only thing that this decrease will produce is to lengthen the portion of the $\rho_a(T)$ curve with the extreme slope. It is quite well known, however, that the original curve length can be recovered through a simple reduction of the thickness h_3 by the same factor c. In other words, any changes in ρ_3 and h_3 which maintain the original conductance h_3/ρ_3 and which satisfy the "high contrast" requirements (ρ_2/ρ_3 and $\rho_4/\rho_3 \geqq 10$), yield the same response function $\rho_a(T)$. This is shown graphically in Fig. 2. The same remarks also apply to the phase response, plotted as ϕ in degrees vs. $\log_{10} T$, as there is again an extremal negative slope which may approach -65.96 when $\rho_3/\rho_2 \to 0$.

Therefore, $\rho_a(T)$ and $\phi(T)$ data with *negative* slopes close to the limiting values consitute a typical trade-off situation from which the only conclusions that can be drawn are upper bounds for the layer thickness and resistivity, and a fairly reliable value for the layer conductance h_3/ρ_3. If there is no independent information as to the value of either ρ_3 or h_3, neither parameter can be determined separately. It also follows from this that the depth to the underlying resistor cannot be deduced from the MT sounding alone.

The second situation which we should like to consider appears at first to be just the opposite of the previous one, but it will lead to conclusions which are not simply "opposite". Here two conducting layers sandwich a highly resistive formation, as with the top three layers in the second example, pertaining to Figs. 4, 5 and 11. If ρ_2/ρ_1 and $\rho_2/\rho_3 \geqq 10$, and if h_2 is again sufficiently thick, $\rho_a(T)$ and $\phi(T)$ will approach their extreme *positive* slopes in a given range of periods, here $T = 70$–200 s,

$$d \ln \rho_a(T)/d \log_{10} T \to 2.303, \quad d \phi(T)/d \log_{10} T \to 65.96.$$

In this situation it becomes impossible to determine ρ_2, except by specifying a lower limit. The length of the steeply sloping curve, on the other hand, is controlled by the layer thickness h_2 which is thereby determined with a high degree

Table 6. *Trade-off matrix* for station NEW (data courtesy of Jones and Hutton, 1979). Apparent resistivities are given in Ωm and thicknesses in km. The values of ε are also given; they are close to $1.10\,\varepsilon_0$, except when a bound is reached, in which case they are usually close to ε_0

ε_- (10^{-3})	ρ_4	h_3	ρ_3	h_2	ρ_2	h_1	ρ_1		ρ_1	h_1	ρ_2	h_2	ρ_3	h_3	ρ_4	ε_+ (10^{-3})
59.71	36.9	262	699	30.1	70.1	27.5	<u>294</u>	$\rho_1 = 10^4$	<u>10^4</u> 13.5	96.5	49.0	626	271	35.3	54.34
59.95	43.7	211	10^4	86.1	126	<u>8.14</u>	10^4	$h_1 = 13.5$	286	<u>37.7</u>	16.3	5.79	682	273	44.0	59.99
59.00	20.0	346	396	0.0323	<u>0.100</u>	26.3	10^4	$\rho_2 = 96.5$	10^4	8.86	<u>128</u>	85.8	6730	214	48.1	59.47
59.45	10.9	341	375	<u>0.0266</u>	0.100	31.0	409	$h_2 = 49.0$	10^4	9.11	124	<u>88.7</u>	10^4	233	20.1	59.19
59.62	5.03	327	<u>342</u>	26.7	71.7	16.1	10^4	$\rho_3 = 626$	10^4	11.9	108	70.2	<u>10^4</u>	202	63.1	55.11
59.74	219	<u>111</u>	10^4	60.0	104	12.5	10^4	$h_3 = 271$	10^4	15.9	78.5	32.4	446	<u>401</u>	0.533	59.67
56.38	<u>0.100</u>	326	498	44.4	92.5	13.8	10^4	$\rho_4 = 35.3$	10^4	13.5	98.7	54.0	1730	131	<u>260</u>	60.15

$$\varepsilon_0 = 54.34 \cdot 10^{-3}$$

AHAUSEN

4-LAYER. $\varepsilon_\rho/\varepsilon_\phi/\varepsilon$ ×1000 : 27/23/25. 3
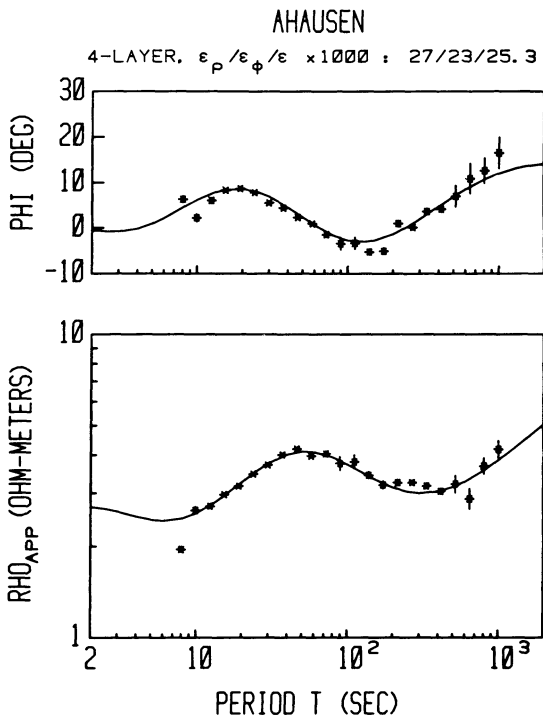

Fig. 4. MT data for station AHA (data courtesy of Jödicke, 1980a) and best-fitting four-layer response (cf. Tables 3 or 4)

of certainty. When ρ_2/ρ_1 is made very large the sloping portion will tend toward its high limit and so h_2 will have to be reduced somewhat to effect the required levelling of the $\rho_a(T)$ curve. If, however, one tries to model the data with the smallest possible ratio ρ_2/ρ_1 the thickness h_2 will have to be increased slightly to produce the levelling off at the same value of $\rho_a(T)$. But unlike what was observed in the previous example, there is only a weak trade-off relation between resistivity ρ_2 and thickness h_2. All we observe in Fig. 5 and Table 4 is that h_2 is at the upper end of its range (about 6 km) when ρ_2 is close to its low bound (about 7.5 Ωm), whereas h_2 drops to 3.8 km when $\rho_2 \to \infty$. Evi-

dently this second situation leads to an entirely different trade-off relationship than the first one. The layer resistivity is given only by a lower bound, but its thickness is determined with rather high accuracy. It is easy to observe with layers no. 2 of the first and second examples and layer no. 3 of the third one (Tables 2, 4, and 6), that the thickness range of such a resistive layer usually spans a factor of about two, and that thick layers always correspond to the lowest permitted resistivities.

Another trade-off situation seems to relate the resistivities of adjacent layers. In the third example (Table 6) it can be observed that when ρ_3 is high, ρ_2 and ρ_4 are generally high too. The same is true for the relation between ρ_3 and ρ_4 in the second example (Table 4). This means that the resistivity contrasts are often as important as the absolute values of the resistivities.

More obvious is the relationship between the thickness of a layer and the resistivity of adjacent layers. If a layer is made as thick as possible, it is likely that the next deeper layer will require a greater resistivity contrast, in order to counteract the decrease in curvature that the thick layer engenders. This can be seen clearly in Tables 2 and 4, where the largest h_2 are coupled with the lowest ρ_3. In Table 6 the largest h_3 are strongly correlated with low ρ_4.

Choosing the Correct Number of Layers

In the preceeding sections the importance of modelling with the correct number of layers has been stressed on several occasions. Once again this is a problem whose answer depends decisively on the availability of independent information about the structure under study. Let us begin with the most common situation, where the only information available is the MT sounding data. Under these circumstances several reasons can be invoked which emphasize the importance of choosing the correct number n_0 of layers with which to model the data. Suppose n_0 has been determined, as for the first three structures chosen as examples (Figs. 1, 4 and 6). It is well known that any number of thin layers can be added to the structures without spoiling or improving the fit significantly. This is clearly seen in
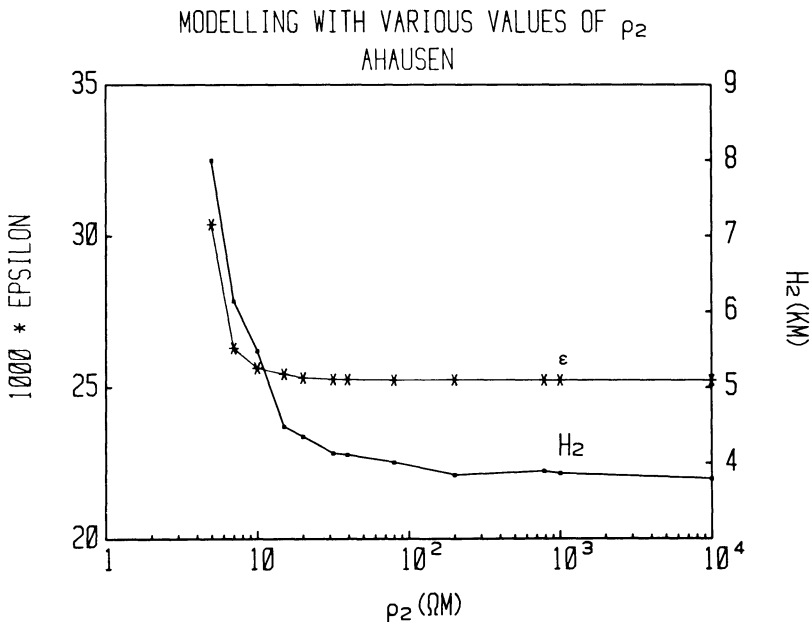
MODELLING WITH VARIOUS VALUES OF ρ_2
AHAUSEN

Fig. 5. Trade-off relationship between ρ_2 and h_2 for station AHA (cf. Fig. 4)
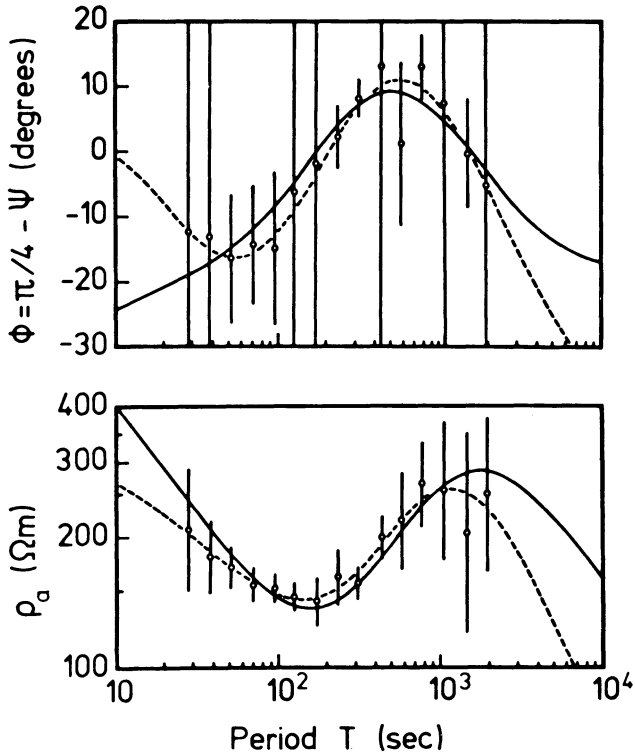
Fig. 6. MT data for station NEW (data courtesy of Jones and Hutton, 1979). The solid line corresponds to the best-fitting model (cf. Tables 5 or 6). The dashed lines are the responses of the best-fitting models to, respectively, the $\rho_a(T)$ data or the $\phi(T)$ data (cf. Fischer and Le Quang, 1981)

Fig. 11. Adding these extra layers is unjustified because it is equivalent to attributing more information to the data set than it actually contains. Good data often appear as highly correlated, but a high correlation implies a reduction of the number of degrees of freedom. In other words, good data can generally be accounted for well with few layers.

But there is another danger in modelling with too many layers. As was shown by Fischer and Le Quang (1981), in the space of model parameters with the correct dimensions $2n_0-1$, the absolute minimum ε_0 occurs at a clearly identifiable isolated point: there are no neighbouring minima and no clusters of local minima. But these statements may well not remain true in a space expanded into more dimensions. The added layers represent more degrees of freedom and with these one moves into the sphere of the so-called "ill-posed problems", whose solution is unstable against minute changes in the data (Tikhonov and Arsénine, 1974). An analogous situation occurs in linear algebra, when the determinant of a system of equations becomes very small, or even vanishes. To render the problem regular again it is necessary to stipulate auxiliary restrictive conditions (add more equations to compensate for the excess of variables). In model space the extra layers correspond to additional dimensions. It then becomes possible to move away from the original well-defined minimum into directions at right angles to all the former dimensions, and in these new directions the original minimum is ill-defined.

Modelling with too few layers has its pitfalls too. Above all it means that the modelling process becomes, right from the start, unable to extract all of the information contained in the data. A further very undesirable consequence of modelling with too few layers is the following. Whereas we were
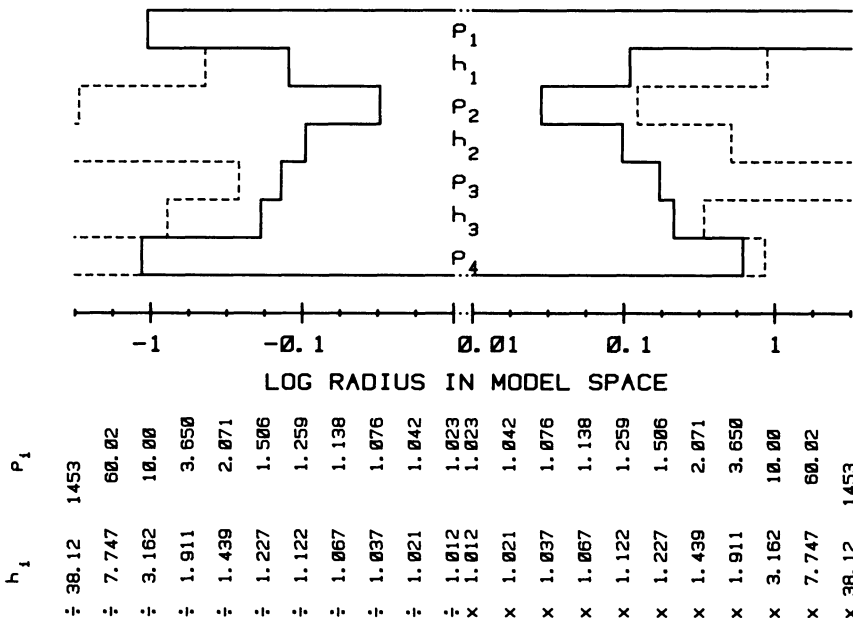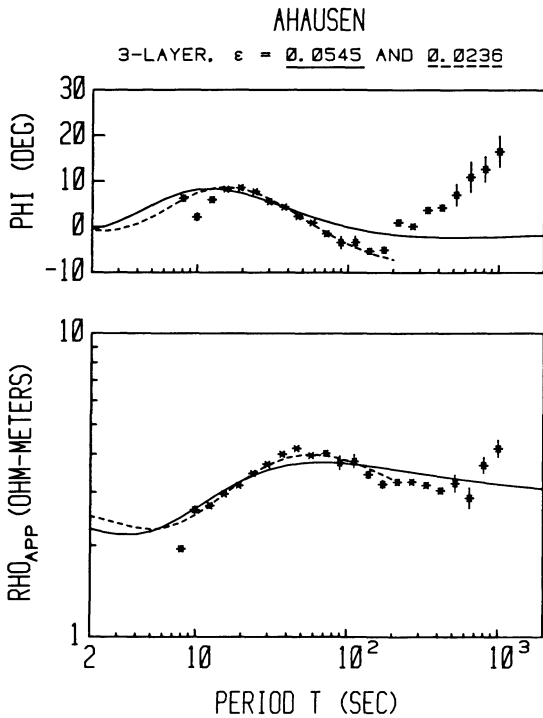

Fig. 7. Trade-off diagram for station NEW (cf. Fig. 6). The limiting parameter values are given along the abscissa. The solid lines correspond to the information contained in the *partial sensitivity matrix,* whereas the dashed lines correspond to the underlined data of the *trade-off matrix*

AHAUSEN
3-LAYER. ε = 0.0545 AND 0.0236

AHAUSEN
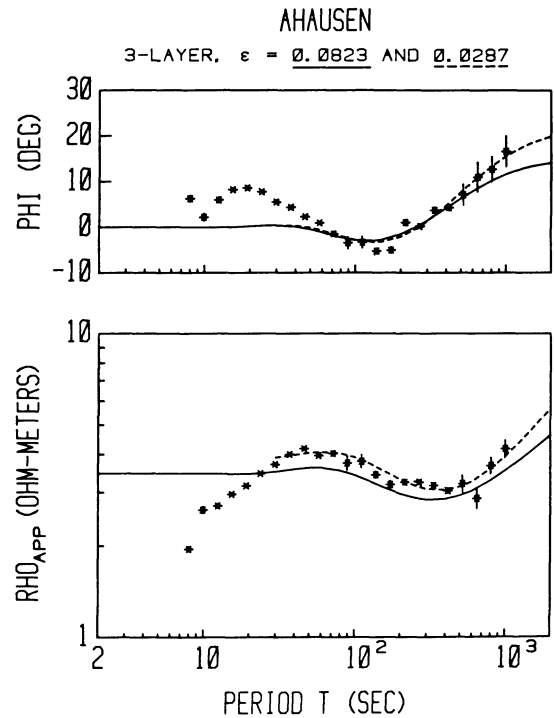### 3-LAYER. ε = 0.0823 AND 0.0287

Fig. 8. Best-fitting three-layer response to the AHA data (cf. Fig. 4). The solid line attempts to fit the entire data set with a three-layer model at the top of the structure. The fit is poor because the minimization routine tries to avoid large misfits also at the long periods. The minimum of ε is therefore shallow. If the data at long periods are ignored the fit improves dramatically (*dashed curve*) and ε exhibits a much deeper minimum

Fig. 9. Best-fitting three-layer response to the AHA data (cf. Fig. 4). The solid line attempts to fit the entire data set with a three-layer model at the bottom of the structure. The fit is poor because the minimization routine tries to avoid large misfits also at the short periods. The minimum of ε is therefore shallow. If the data at short periods are ignored the fit improves dramatically (*dashed curve*) and ε exhibits a much deeper minimum

generally unable to find, in the space with the correct dimensions $2n_0-1$, other minima of ε besides the absolute minimum ε_0 (Fischer and Le Quang, 1981), it is evident that in a space with too few dimensions such multiple minima exist, even though they will be shallow and separated by large distances. Consider our second example; this data set should be modelled with four layers (Fig. 4). When attempting to model with three layers it is clear that the minimization process may try to fit either the top three layers or the bottom three. As seen in Figs. 8 and 9 the minimization routine converges toward two well-defined structures, each of which corresponds to an isolated minimum in parameter space, with a large separation between the two.

The seeming uniqueness of the solution when n is chosen at its correct value n_0, is evidently lost when $n \neq n_0$. With $n < n_0$ separate minima of ε at large distances from each other are an obvious consequence. For $n > n_0$ a cluster of minima is likely near the original minimum of ε, but in directions of the added dimensions.

Choosing the correct value of n_0 is perhaps not always as straightforward as the first three examples cited suggest (Fig. 11). An illustration of the difficulties one may encounter are given by the data set RABE shown in Fig. 10. Modelling these data with structures comprising 2–6 layers yields the $\varepsilon_0(n)$ function shown in Fig. 11. Our contention is that if no other information is available the RABE data set does not give definite evidence for the presence of more than three layers of different conductivity. The existence of more layers can only become justified if additional fac-

tors support it, like MT data from a series of soundings along a profile of which RABE is just a single bracketed site.

As was said at the beginning of this section, the availability of independent information concerning the structure under MT study may completely change the problem of determining the appropriate number of layers. The additional information may well require more layers, but is likely at the same time to introduce constraints by specifying the resistivity or thickness of certain layers. Postulating more layers increases the *trade-off volume*, but the additional constraints delimit a sub-class of models within the larger volume. The more stringent the constraints, the smaller the sub-class volume and the greater the likelihood that there will be a single isolated minimum of ε within the sub-class.

Conclusions

The 1 D/MT modelling routine developed recently by Fischer and Le Quang (1981) has made it possible to investigate the entire range of model parameter variations which are compatible with a predetermined degree of fit between model response and measured data. This range of possible or permitted models can be represented as a volume in parameter space, the *trade-off volume*. The enclosing *trade-off surface* is singly connected but usually has a complicated topography. It can be reasonably well characterized by the *partial sensitivity matrix*, which gives the intersections with the parameter axes, and the *trade-off matrix*, which specifies the coordinates of the extreme extensions in the directions

3-LAYER AND 6-LAYER

$\varepsilon_\rho/\varepsilon_\phi/\varepsilon \times 1000$: $\underline{45/20/34.8}$
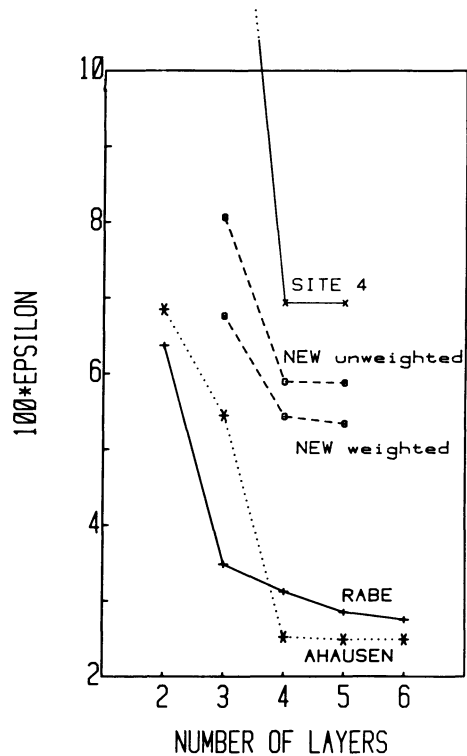
$\underline{37/12/27.5}$
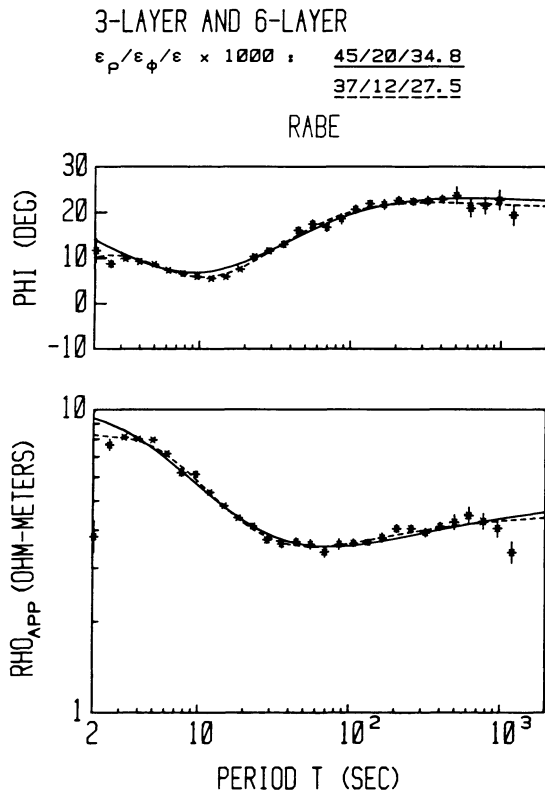
RABE

Fig. 10. MT data set for station RABE (data courtesy of Jödicke, 1980b). The solid curve corresponds to the best-fitting three-layer model. The dashed curve corresponds to the best-fitting six-layer model. The improvement over the three-layer fit is only slight (cf. Fig. 11)

Fig. 11. Standard deviation ε_0 of the best-fitting models, for the various MT data sets considered, as a function of the number of layers postulated. In most instances there is no difficulty identifying a unique correct choice n_0

of the parameter axes. The extensions in other directions could likewise be investigated by the same modelling routine. But the *trade-off matrix* not only states the extreme range a given parameter can assume, it also specifies the trade-off conditions to which the remaining model parameters have to be subjected to achieve this range.

The incidence of the choice of the number of layers on the modelling process has been looked at in detail. The importance of a correct choice to insure a unique best-fit have been stated, especially as regards over-fitting, i.e., attempting to model with too many layers. If reliable prior geological knowledge is available, this knowledge should be used as it reduces the range of permitted solutions to a sub-class among all the solutions comprising the *trade-off volume*. This is especially important if prior information requires more layers than can be inferred from the MT data alone: the *trade-off volume* increase resulting from the added layers must be counteracted through reduction to a sub-class, by pegging some layer thicknesses or resistivities, since otherwise a unique best-fitting solution cannot be expected.

Since the *trade-off volume* encompasses all the models acceptable within a pre-set standard deviation ε, and since ε is given as sum of the squares of the individual data misfits, it is clear that the *trade-off volume* also comprises those solutions which tend to give misfits systematically on one side or the other of the data points. This is to be expected. Fortunately it is easy to convince oneself that such systematic deviations over large ranges of the data are impossible for the best-fitting model.

References

Edwards, R.N., Bailey, R.C., Garland, G.D.. Conductivity anomalies: lower crust or asthenosphere? Phys. Earth Planet. Inter. **25**, 263–272, 1981

Eichler, K.. Inversion eindimensionaler Magnetotellurik-Daten mit Hilfe eines Optimierungsverfahrens, Diploma thesis, Department of Geophysics, University of Münster, Federal Republic of Germany, 1980

Fischer, G., Schnegg, P.-A., Peguiron, M., Le Quang, B.V.. An analytic one-dimensional magnetotelluric inversion scheme. Geophys. J. R. Astron. Soc. **67**, 257–278, 1981

Fischer, G., Le Quang, B.V.. Topography and minimization of the standard deviation in one-dimensional magnetotelluric modelling. Geophys. J. R. Astron. Soc. **67**, 279–292, 1981

Hobbs, B.A.. The electrical conductivity of the Moon: an application of the inverse theory. Geophys. J. R. Astron. Soc. **51**, 727–744, 1977

Hobbs, B.A.. Automatic model finding for the one-dimensional magnetotelluric problem. Geophys. J. R. Astron. Soc. **68**, 253–264, 1982

Inman, J.R.. Resistivity inversion with ridge regression. Geophysics **40**, 798–817, 1975

Jackson, D.D.. Marginal solutions to quasi-linear inverse problems in geophysics: the edgehog method. Geophys. J. R. Astron. Soc. **35**, 121–136, 1973

Jödicke, H.: Magnetotellurik Norddeutschlands-Versuch einer Interpretation. Protokoll über das Kolloquium "Elektromagnetische Tiefenforschung", Berlin-Lichtenrade, 271–288, April 1–3, 1980a

Jödicke, H.: Magnetotellurik-Ergebnisse im Rheinischen Schiefergebirge. Protokoll über das Kolloquium "Elektromagnetische Tiefenforschung", Berlin-Lichtenrade, 323–328, April 1–3, 1980b

Johansen, H.K.: A man/computer interpretation system for resistivity sounding over a horizontally stratified earth. Geophys. Prosp. 25, 667–691, 1977

Jones, A.G., Hutton, R.: A multi-station magnetotelluric study in southern Scotland – II. Monte-Carlo inversion of the data and its geophysical and tectonic implications. Geophys. J. R. Astron. Soc. 56, 351–368, 1979

Jupp, D.L.B. and Vozoff, K.: Stable iterative methods for the inversion of geophysical data. Geophys. J. R. Astron. Soc. 42, 957–976, 1975

Lanczos, C.: Linear differential operators. London: D. Van Nostrand, 1961

Larsen, J.C.: A new technique for layered-earth magnetotelluric inversion. Geophysics 46, 1247–1257, 1981

Oldenburg, D.W.: One-dimensional inversion of natural source magnetotelluric observations. Geophysics 44, 1218–1244, 1979

Parker, R.L.: The inverse problem of electrical conductivity in the mantle. Geophys. J. R. Astron. Soc. 22, 121–138, 1970

Parker, R.L.: The inverse problem of electromagnetic induction: existence and construction of solutions based on incomplete data. J. Geophys. Res. 85, 4421–4428, 1980

Parker, R.L., Whaler, K.A.: Numerical methods for establishing solutions to the inverse problem of electromagnetic induction. J. Geophys. Res. 86, 9574–9584, 1981

Rokityansky, I.I.: Geoelectromagnetic investigation of the earth's crust and mantle. Berlin, Heidelberg, New York: Springer-Verlag 1982

Schnegg, P.-A., Le Quang, B.V., Fischer, G.: AMT Untersuchung einer 2D Struktur mit einer Überschiebung. Protokoll über das Kolloquium "Elektromagnetische Tiefenforschung", Neustadt a.W., 55–59, March 22–26, 1982

Shoham, Y., Ginzburg, A., Abramovici, F.: Crustal structure in central Israel from the inversion of magnetotelluric data. J. Geophys. Res. 83, 4431–4440, 1978

Tikhonov, A. and Arsénine V.: Méthodes de résolution de problèmes mal posés. Moscow: Editions MIR 1974 (original edition in Russian)

Vozoff, K. and Jupp, D.L.B.: Joint inversion of geophysical data. Geophys. J. R. Astron. Soc. 42, 977–991, 1975

Wiggins, R.A.: The general linear inverse problem: implication of surface waves and free oscillations for earth structure. Rev. Geophys. Space Phys. 10, 251–285, 1972

Note Added in Proof

We have been able to show that our minimizing routine is equally applicable to 1D Wenner and Schlumberger sounding data. As a consequence, equivalent trade-off conditions can be formulated for such data sets, and our discussion relating to the correct number of layers with which to model applies without modification to such sets.